AN IN-SITU YOUNG'S MODULUS MEASUREMENT TECHNIQUE FOR NUCLEAR POWER PLANTS USING TIME-FREQUENCY ANALYSIS

YOUNG-CHUL CHOI[1], DOO-BYUNG YOON[1], JIN-HO PARK[1] and HYU-SANG KWON[*2]
[1]Advanced Reactor Tech. Korea Atomic Energy Research Institute
150 Duckjin-dong Yuseong-gu, Daejeon, Korea
[2]Korea Research Institute of Standards and Science
1 Doryong-dong Yuseong-gu, Daejeon, Korea
[*]Corresponding author. E-mail : hyusang@kriss.re.kr

Received November 30, 2007
Accepted for Publication October 26, 2008

Elastic wave is one of the most useful tools for non-destructive tests in nuclear power plants. Since the elastic properties are indispensable for analyzing the behaviors of elastic waves, they should be predetermined within an acceptable accuracy. Nuclear power plants are exposed to harsh environmental conditions and hence the structures are degraded. It means that the Young's modulus becomes unreliable and in-situ measurement of Young's modulus is required from an engineering point of view. Young's modulus is estimated from the group velocity of propagating waves. Because the flexural wave of a plate is inherently dispersive, the group velocity is not clearly evaluated in temporal signal analysis. In order to overcome such ambiguity in estimation of group velocity, Wigner-Ville distribution as the time-frequency analysis technique was proposed and utilized. To verify the proposed method, experiments for steel and acryl plates were performed with accelerometers. The results show good estimation of the Young's modulus of two plates.

KEYWORDS : Young's Modulus, Poisson's Ratio, Wigner-Ville Distribution, Flexural Rigidity, Group Velocity, Lamb Wave, Accelerometer

1. INTRODUCTION

In non-destructive testing methods, elastic wave has been well known as one of the most popular and widely used tools alongside vibration, ultrasonic tests, and acoustic emissions, etc. Because it is generated or reflected by mechanical means such as shocks, fatigues, or sudden discontinuities, the health and safety of solid structures or plants could be monitored by detecting the wave propagations [1-6]. Pipes, tubes, and tanks are well known as areas of concern, and nuclear power plants are obviously composed of those items.

In using elastic waves for these purposes, the so-called time-of-flight is essential to localize the targets without doubt. In addition, modal parameters such as resonant frequencies and mode shapes are sometimes useful in characterizing the changes of structures in mechanical means. It is well known that these elastic behaviors in a structure depend highly on its own mechanical properties and dimensions as well as source characteristics, and hence these properties should be identified in the first place. As a result, the elastic properties, generally given as constants, are prerequisite for elastic behavior analysis.

The elastic properties of solid materials are of considerable significance to both science and technology. Because the elastic properties describe the mechanical behavior of materials, their measurement is also important for engineering purposes. Indeed, dynamical measurements of the elastic properties have been established to provide the relevant data. Dynamical methods offer more advantages, such as accuracy and applicability to small samples under various conditions than do static tensile, compressive and torsional tests [7-9]. However, these well established and standardized test methods require well designed test specimens and equipment with laboratory environments, and they have shortcomings in some engineering applications. As a matter of fact, in-situ measurements of elastic properties are highly desirable in numerous test conditions.

Because nuclear power plants are exposed to harsh environmental conditions like high temperature, high pressure, high speed flow, and moreover radioactivity, the structures are sure to be degraded and deformed in nature as they operate over a long time. This means that the elastic properties, which must be determined well when the plant is designed and built at first, become

unreliable. As the plant is degraded, non-destructive tests for safety monitoring are required much more and, consequently, in-situ measurements of elastic properties are strongly desirable from an engineering point of view [10-12].

Without loss of generality, most structures of interest in the nuclear power plants are considered as plates or shells in the frequency range of interest and thus the flexural behaviors are mainly considered. The flexural wave, or so-called Lamb wave, is governed by well known wave equations with a constant of flexural rigidity which should be measured. The flexural rigidity is composed of elastic constants of Young's modulus and Poisson's ratio which are obtained in the same manner. As a consequence, Young's modulus is deduced in assumption of invariable Poisson's ratio.

As a dynamical method, the speed of wave propagation is available by measuring the time delay between two distant accelerometers [13]. However, the flexural wave is inherently dispersive different to simple compressive or shear waves and hence the waveform is spread in propagation. To overcome the ambiguity in time delay estimation, a novel signal processing technique was first proposed in this article. Time-frequency analysis based on Wigner-Ville distribution shows obviously dispersive wave propagating characteristics as is well known and, according to the results, the exact time delay can be clearly estimated from distinguished waves via the time-frequency spectrum. It induces Young's modulus of thin-wall structure in the nuclear power plant as simply measurable in-situ within sufficient accuracy.

Experiments validated the proposed method well. Flat homogeneous plates of steel and acryl were tested for the convenience of experiments. As expected, the proposed method works well and is available for practical use without loss of generality. The error due to the variation of Poisson's ratio was also analyzed.

2. THEORETICAL BACKGROUND

When a shock is applied to a structure, shock waves travel along the structure,where the transmission velocity varies according to the qualities of a material. For example, when a material is hard, the transmission velocity of the waves is high, and when a material is soft, the velocity is low. So, if we measure the transmission velocity of the shock waves, we can estimate the physical properties of a material. In this chapter, we discuss the theoretical relationship between the transmission velocity of the shock waves and the flexural rigidity. We also propose a method to calculate the Young's modulus.

2.1 The Relationship between a Group Velocity and the Flexural Rigidity in a Plate Model [18]

As shown in Fig. 1, when shock is applied to a plate

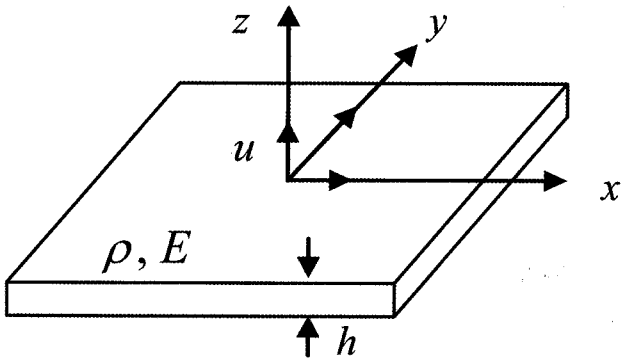

Fig. 1.A Plate Model Used Here, where h is the Thickness, ρ is the Density, and E is the Young's Modulus

which consists of the same material and has uniform thickness, a Lamb wave occurs. The traveling velocity of the Lamb wave correlates with what kind of material the rigid body consists of, how thick it is, and the frequency of the wave, and it can be calculated analytically by the Rayleigh-Lamb equation [14-15]. The traveling velocity of A_0 wave is given by

$$\frac{\tan(\sqrt{1-\varsigma^2}\cdot kh)}{\tan(\sqrt{\xi^2-\varsigma^2}\cdot kh)} = -\frac{(2\varsigma^2-1)^2}{4\varsigma^2\sqrt{1-\varsigma^2}\sqrt{\xi^2-\varsigma^2}} \tag{1}$$

Where

$$\varsigma \equiv \frac{C_t}{C_{ph}}, \quad \xi \equiv \frac{C_t}{C_l}$$

$$C_l \equiv \sqrt{\frac{E}{\rho}\times\frac{1-\nu}{(1+\nu)(1-2\nu)}}, \; C_t \equiv \sqrt{\frac{G}{\rho}}$$

h : thickness of plate, E : Young's modulus, ρ : density, ν : Poisson's ratio, C_{ph} :phase speed(ω/k), G : shear modulus, k : wave number, ω : angular velocity, f : frequency

The complete solution of equation (1) is hard to obtain, but a wave's traveling velocity according to the frequency can be obtained by a numerical analysis. Ross suggested a very simple solution which approximates the analytical results above [16]:

$$C_{ph} = C_L' \cdot \sqrt{\frac{1.8\cdot h\cdot f}{C_L' + 4.5\cdot h\cdot f}} \tag{2}$$

Where

$$C_L' = \sqrt{\frac{E}{\rho(1-\nu^2)}} \tag{3}$$

In the case where two or more components of a flexural wave travel simultaneously because of an impact, a combination of these flexural waves gives rise to an envelope distribution. The traveling velocity of the envelope is called a group velocity, i.e. traveling velocity of a wave's energy [17]. The definition of a group velocity is given by

$$C_g \equiv \frac{d\omega}{dk} = d\omega\left[d\left(\frac{\omega}{C_{ph}}\right)\right]^{-1} = C_{ph}^{\ 2}\cdot\left[C_{ph} - \omega\cdot\frac{dC_{ph}}{d(\omega)}\right]^{-1} \quad (4)$$

The complete solution of a group velocity can be obtained by drawing the phase velocity (C_{ph}) value from equation (1) and applying it to equation (4). By using Ross's approximate solution, a group velocity is provided equation (2) and equation (4) as:

$$C_g = \frac{3.6\cdot hf\cdot C_L^{'\,2}}{C_{ph}\cdot(C_L^{'} + 9hf)} \quad (5)$$

Meanwhile, if the wavelength of the flexural wave is much larger than the thickness of a plate, or if the frequency of the flexural wave is low (kh<1), the phase velocity and group velocity can be simply given as

$$C_{ph} \cong \sqrt{\omega}\left(\frac{D}{\rho h}\right)^{\frac{1}{4}} \quad (6)$$

$$C_g \cong 2\cdot\sqrt{\omega}\left(\frac{D}{\rho h}\right)^{\frac{1}{4}} \quad (7)$$

In which the quantity

$$D = \frac{Eh^3}{12(1-\nu^2)}$$

is called the flexural rigidity of the plate, so equation (7) can be rearranged with regards to flexural rigidity:

$$D = \frac{\rho\cdot h}{16\cdot\omega^2}\cdot C_g^4 \quad (8)$$

Equation (8) reveals that we can estimate flexural rigidity if group velocity is known.

2.2 Measuring Group Velocity

It has been proven that the peak magnitude line of the flexural wave in the Wigner-Ville distribution is highly dependent on the group velocity [20]. Therefore, the group velocity can be measured by dividing the difference between the distances from the impact point to a pair of transducers by measuring the time-of-arrival difference between two sensors.

In the one-dimensional case as shown in Fig.2, group velocity equals the arrival time delay between two sensors divided by their distance, i.e. with the distance between the two sensors $\Delta x = x_2 - x_1$ and the corresponding arrival time delay $\Delta t = t_2 - t_1$, the group velocity is given by [20]

$$C_g = \frac{\Delta x}{\Delta t} \quad (9)$$

Therefore, the group velocity can be estimated by measuring arrival time delay Δt. There are many methods for measuring Δt. The conventional method is to find Δt in the time domain. But, it is only applicable if we have high signal-to-noise ratio (SNR). The phase point location technique by using cross correlations [22] can give a more accurate Δt than the conventional time domain analysis. However, it deals with Δt only at a single frequency component which is sensitive to the propagation path and sensor locations. Recently, the time-frequency analysis technique was employed to calculate Δt more exactly.

In this paper, we apply a time-frequency analysis to obtain the arrival time delay between the sensors accurately. In general, there are three time-frequency analysis methods [17-21]: Short Time Fourier Transform, Wavelet, and Wigner-Ville analysis. Of the three methods, we have chosen the Wigner-Ville analysis because of its superior frequency and time resolution. Wigner-Ville distribution is a sort of bilinear TFR (time frequency representation) and is defined as follows:

$$\begin{aligned} W(t,f) &\equiv \int_{-\infty}^{\infty} R(t,\tau)e^{-j2\pi f\tau}d\tau \\ &= \int_{-\infty}^{\infty} z(t-\frac{\tau}{2})z^*(t+\frac{\tau}{2})e^{-j2\pi f\tau}d\tau \\ &= \int Z^*(\omega+\frac{\varphi}{2})Z(\omega-\frac{\varphi}{2})e^{-jt\varphi}d\varphi \end{aligned} \quad (10)$$

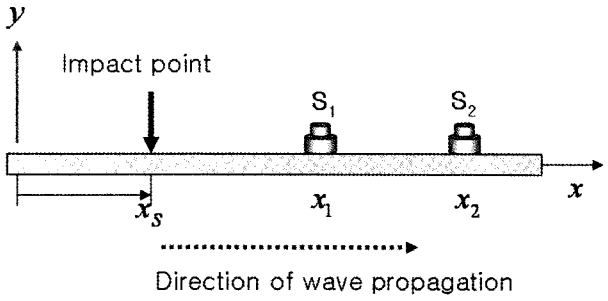

Fig. 2. One-dimensional Experimental Setup for Estimating Group Velocity.

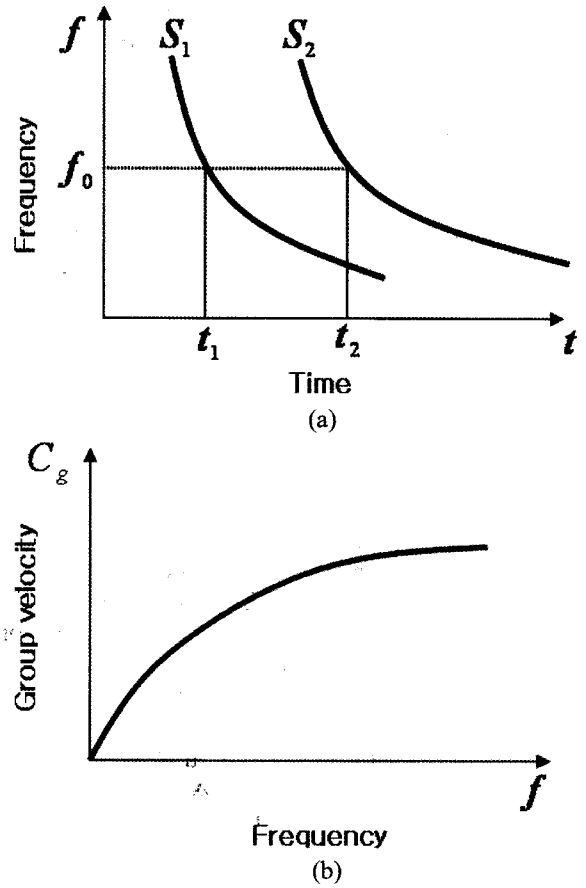

Fig. 3. The Estimation of Group Velocity. (a) In Time-Frequency Domain, Peak Amplitude Lines Corresponding to Two Different Sensors, where S Means a Sensor, Subscripts 1, 2 Denote the Sensor Numbers, and t_1, t_2 are the Arrival Times of the Sensors S_1 and S_2 at a Frequency f_0 Respectively. (b) The Group Velocity Calculated by Equation (9)

where

$$R(t,\tau) = z(t-\frac{\tau}{2})z^*(t+\frac{\tau}{2})$$

is a time dependent autocorrelation function, $z(t)$ is an analytical function of the signal $Z(\omega)$, and a Fourier transform of $z(t)$. That is, the Wigner-Ville distribution is defined as a Fourier transform of the time lag of a time dependent autocorrelation function, and in physical terms, it represents a frequency distribution of the energy of a signal at each time literal.

Fig. 3 explains the method of estimating group velocity by using Winger-Ville analysis. In a dispersive structure, the group velocity of the wave component differs according to the frequency [21]. So, the shape of the peak amplitude lines in the time-frequency domain looks like Fig. 3(a). From the equation (9), the group velocity can be calculated as shown in Fig. 3(b).

2.3 Estimating Young's Modulus

Because flexural rigidity is expressed as ,

$$D = \frac{Eh^3}{12(1-\nu^2)},$$

equation (8) can be derived to be

$$E = \frac{3}{4}\cdot\frac{\rho\cdot(1-\nu^2)}{\omega^2\cdot h^2}\cdot C_g^4 \tag{11}$$

In equation (11), density of the plate (ρ) equals its mass divided by its volume, and Poisson's ratio value (V) ranges from 0.24 to 0.35 for most metals[14]. So, if we can measure a group velocity, the Young's modulus can be obtained.

In order to obtain the Young's modulus from equation (11), the density of a plate and its' Poisson's ratio have to be known beforehand. In the case of most metals, Poisson's ratio ranges from 0.24 to 0.35 [6]. In this section, we discuss how much of on error is induced in the Young's modulus by assuming the Poisson's ratio.

If we let

$$\frac{3}{4}\cdot\frac{\rho}{\omega^2\cdot h^2}\cdot C_g^4$$

be A, equation (11) can be presented simply as

$$E = A\cdot(1-\nu^2) \tag{12}$$

Let the error in assuming the Poisson's ratio be ε, than the Poisson's ratio with an error, V', can be given as

$$\nu' = \nu + \varepsilon \tag{13}$$

It we let the real value of the Young's modulus be E_t and the Young's modulus with an error be E_e, the error in assuming the Young's modulus is given as

$$error = \frac{E_t - E_e}{E_t}\times 100 = \frac{(2\nu+\varepsilon)}{1-\nu^2}\cdot\varepsilon\times 100 \tag{14}$$

Thus, if we let the Poisson's ratio be 0.3, and the real value of the Poisson's ratio ranges from 0.25 to 0.35, the maximum error in assuming the Young's modulus is 3.6 %. This is within the permitted error range, so it is acceptable to let the Poisson's ratio, V be 0.3 in equation (11).

3. EXPERIMENT

So far, we have discussed a theoretical method for estimating the Young's modulus by measuring a group velocity. In this chapter, we discuss the SUS304 and acryl plate experiments which are used to test the theoretical contents.

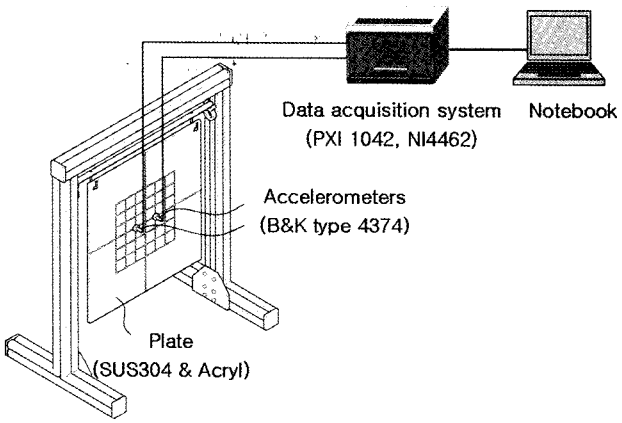

Fig. 4. Experimental Setup for Estimating the Young's Modulus with a Sampling Frequency of 200 kHz

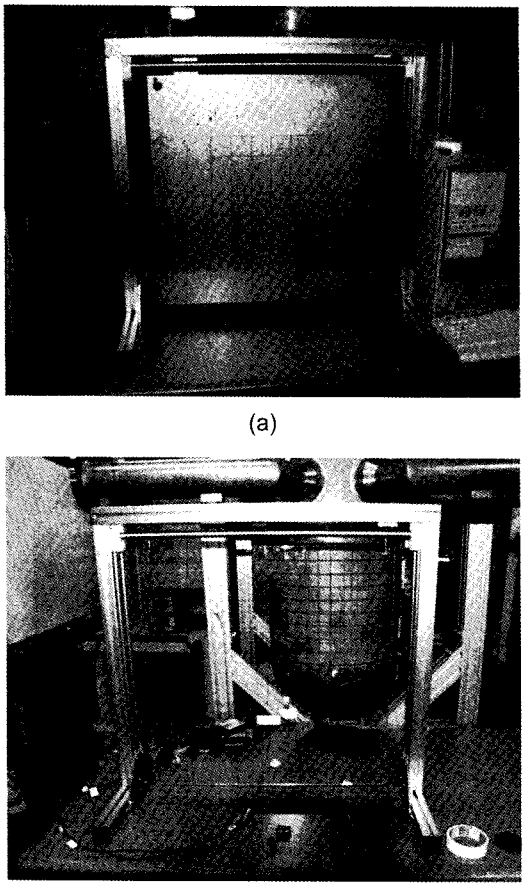

Fig. 5. A Picture of (a) 600 mm × 600 mm × 2 mm SUS304 Plate, (b) 600 mm × 600 mm × 10 mm Acryl Plate

3.1 Experimental Setup

Fig. 4 shows the experimental setup for estimating the Young's modulus. We used two accelerometers of B&K type 4374. The distance between the sensors is 100mm and the impact is applied to a point which is separated from sensor 1 by 100mm and which is on the extended line where the two sensors are attached. The impact hammer used is made by KAERI. The signal was stored by a data acquisition system (NI 4462 board) with 200 kHz sampling.

600 mm × 600 mm × 2mm SUS304 plate and 600 mm × 600 mm × 10mm acryl plate are used as shown in Fig. 5, where the mass of acryl plate is 3.9 kg and density is 1083 kg/m^3.

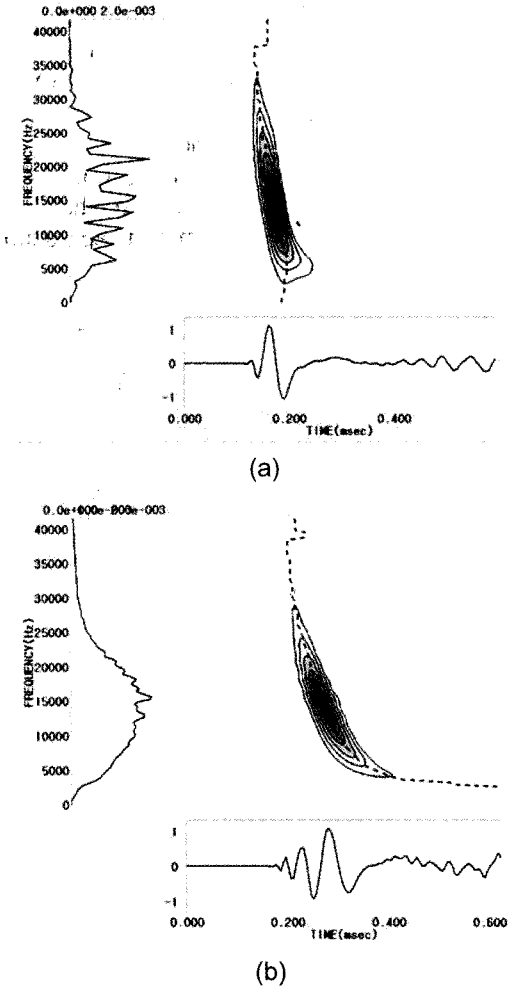

Fig. 6. Wigner-Ville Analysis Result of a SUS304 Plate for (a) Sensor 1, and (b) Sensor 2 where the Dotted Line Means Maximum Value at the Wigner-Ville Distributions

3.2 Experimental Results

3.2.1 SUS Plate

Fig. 6 shows the acceleration signals of two accelerometers respectively and their Wigner-Ville distributions. The figures on the left are their corresponding power spectra.

As shown in Fig. 6, if the distribution characteristic is that the high-frequency components arrive early, the distribution curve appears more clearly when observed farther from the impact point.

It is difficult to obtain the arrival time delay between the two accelerometers from the acceleration signals in the time domain, but if we use the maximum line in the Wigner-Ville distribution in the time-frequency domain, the arrival time delay according to the frequency can be found easily, as shown in Fig. 7. The distance between the two sensors is 100mm, so from equation (9), the group velocity according to the frequency can be estimated as is shown in Fig. 6.

The thickness of the plate is 2 mm, the size is 600 × 600 mm and the volume is 720×10^3 mm^3. The mass is 5.7 kg, so the density is 7930 kg/m^3. Thus, if we let the Poisson's ration value be 0.3 and insert the group velocity from Fig. 7 into equation (11), we can obtain the Young's modulus as shown in Fig. 7.

As shown in Fig. 6, the frequency area which reveals a good S/N ratio is from 5 kHz to 10 kHz, so in Fig. 8, the same frequency area is important. Therefore, the estimated Young's modulus from the experiment is approximately 200 GPs. The Young's modulus of SUS304 used in this experiment is 205 GPs [14], so the estimated value coincides with the reference value within a 2.4 % error range.

3.2.2 Acryl Plate

The experiment is the same as the case of SUS304 plate, and as a result, the distribution curve in the time-frequency domain is obtained as shown in Fig. 9.

Group velocity is obtained from the distribution curves

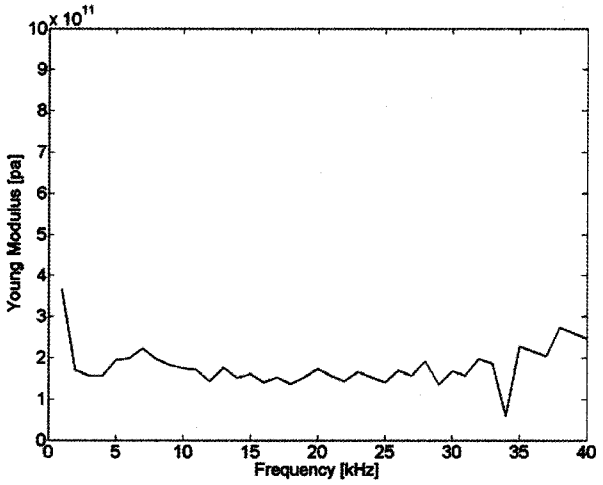

Fig. 8. Estimated Young's Modulus for the SUS 304 Plate at the Frequency Region which Reveals a Good Signal to Noise Ratio

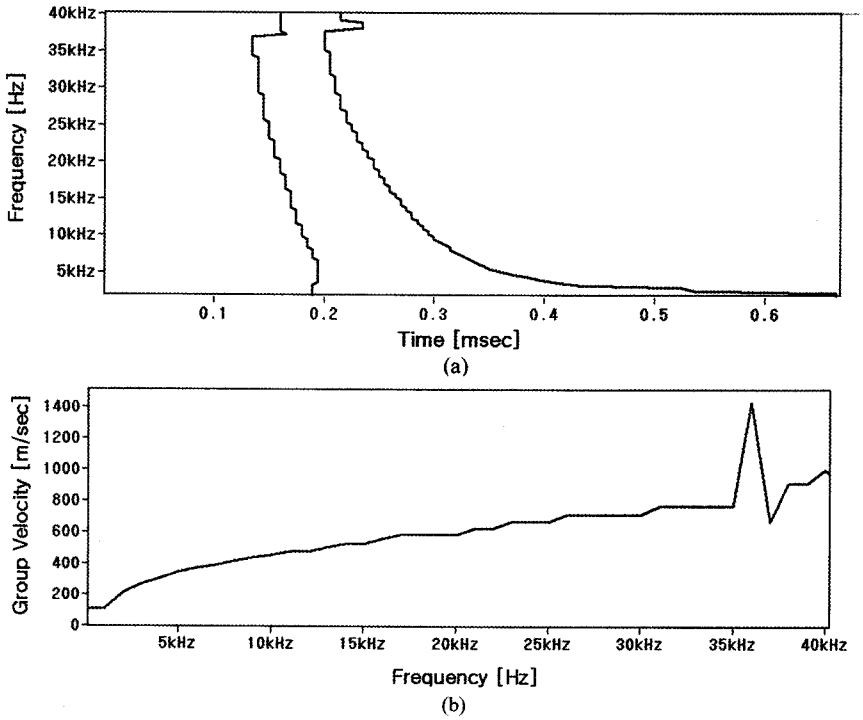

Fig. 7. (a) Maximum Line in the Wigner-Ville Distribution in Case of SUS Plate, (b) Estimated Group Velocity

of each sensor in Fig. 10, and the Young's modulus is estimated by inserting the obtained group velocity into equation (11). Fig. 11 shows the estimation result as approximately 2.3 GPa. As shown in Fig. 9, the frequency area reveals a good S/N ratio is from 5 kHz to 10 kHz, so the estimated Young's modulus is an average value from this area. The Young's modulus of the acryl used is between 2.2 GPa and 3.8 GPa, so it corresponds well with the estimated value from the proposed experiment.

4. CONCLUSION

In order to estimate the Young's modulus, it is necessary to fabricate a uniform test sample and apply it to a tensile test. This paper proposed a method for estimating the Young's modulus in-situ by measuring a group velocity in metal components with accelerometers without fabricating a test sample. This method can be successfully applied to the plate-like structures having uniform density

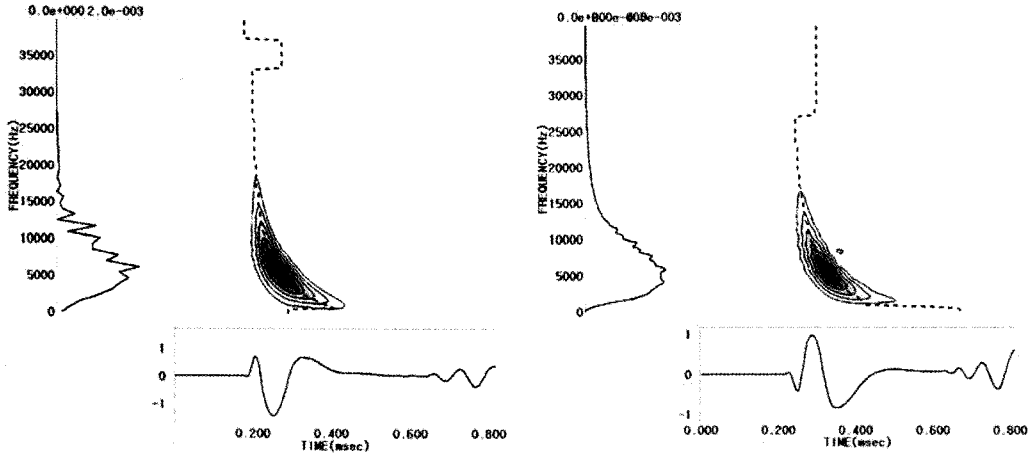

(a) (b)

Fig. 9. Wigner-Ville Analysis Result of an Acryl Plate for (a) Sensor 1, (b) Sensor 2 where the Dotted Line Means Maximum Value at the Wigner-Ville Distributions

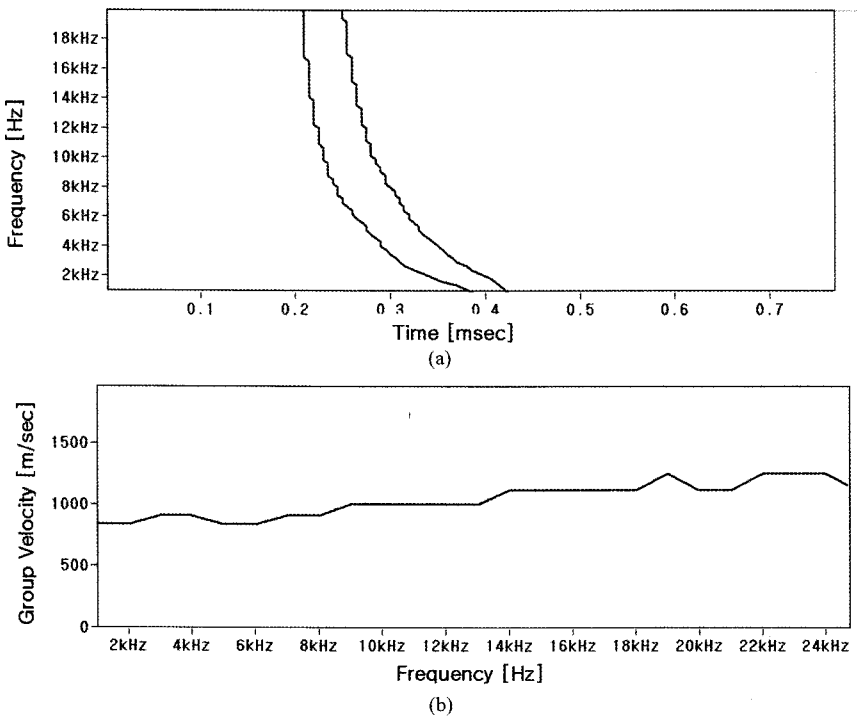

Fig. 10. (a) Maximum Line in the Wigner-Ville Distribution in Case of Acryl Plate, (b) Estimated Group Velocity

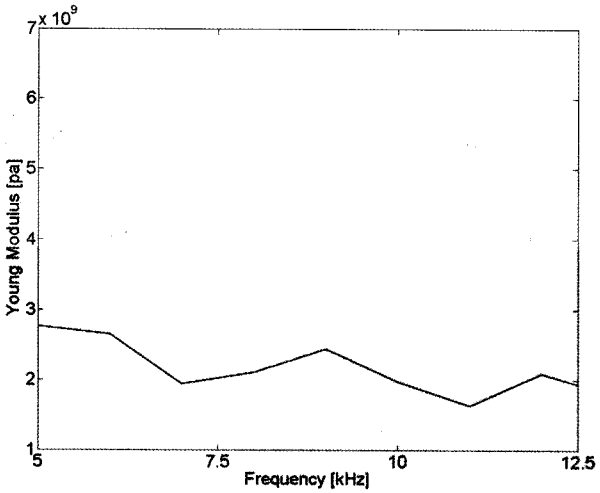

Fig. 11. Estimated Young's Modulus for Acryl Plate at the Frequency Region which Reveals a Good Signal to Noise Ratio

and thickness. In this paper, we extend the application to the Young's modulus estimation for practical uses in engineering applications. In use of time frequency analysis.

ACKNOWLEDGEMENT

This work is supported by Ministry of Commerce, Industry and Energy.

REFERENCES

[1] Designation: E 1876-07, "Standard Test Method for Dynamic Young's Modulus, Shear Modulus, and Poisson's Ratio by Impulse Excitation of Vibration," *ASTM International.*

[2] Designation: E 1875-00, "Standard Test Method for Dynamic Young's Modulus, Shear Modulus, and Poisson's Ratio by Sonic Resonance," *ASTM International.*

[3] Designation: C 848-88 (Reapproved 2006), "Standard Test Method for Young's Modulus, Shear Modulus, and Poisson's Ratio for Ceramic Whitewares by Resonance," *ASTM International.*

[4] Designation: C1198-01, "Standard Test Method for Dynamic Young's Modulus, Shear Modulus and Poisson's Ratio for Advanced Ceramics by Sonic Resonance," *ASTM International.*

[5] Designation: C1259-01, "Standard Test Method for Dynamic Young's Modulus, Shear Modulus, and Poisson's Ratio for Advanced Ceramics by Impulse Excitation of Vibration," *ASTM International.*

[6] Yong-Moo Cheong, Joo-Hag Kim and Hyun-Kyu Jung, "Dynamic elastic constants of weld HAZ of SA 508 CL.3 steel using resonant ultrasound spectroscopy," *15th world conference on non-destructive testing 15-16 October 2000 in Rome*, (2000).

[7] Designation: E111-04, "Standard Test Method for Young's Modulus, Tangent Modulus, and Chord Modulus," *ASTM International.*

[8] Sang-Hyun Kim and James G Boyd, "A new technique for measuring Young's modulus of electroplated nickel using AFM", *Measurement Science & Technology*, **17**, p.2343-2348 (2006).

[9] M. Radovic, E. Lara-Curzio, L. Riester, "Comparison of different experimental techniques for determination of elastic properties of solids", *Materials Science and Engineering* A368, p.56-70 (2004).

[10] B.K. Shah, "Irradiation and thermal induced material ageing degradation of nuclear components", *IAEA-RCA Training course on in-service inspection of research reactors*, January 21-February 1, Mumbai, India, p.29-34 (2002).

[11] K.C. Sahoo, "Material degradation of research reactor components", *IAEA-RCA Training course on in-service inspection of research reactors*, January 21-February 1, Mumbai, India, p.35-54 (2002).

[12] P.K. De, "Environmental degradation of materials for research reactors", *IAEA-RCA Training course on in-service inspection of research reactors*, January 21-February 1, Mumbai, India, p.55-67 (2002).

[13] C.-H Sohn, Y.-C. Choi, et al. 2006, "Monitoring Pipe Thinning using time-frequency Analysis", *The Korean Society for Noise and Vibration Engineering.* **16**, No.12, p.1224-1230 (2006).

[14] L. Cremer and M.Heckl, Structure-Borne Sound, Springer-Verlag Berlin Heidelberg New York London Paris Tokyo, p.101 (1998).

[15] I.A. Viktorov, Rayleigh and lamb waves, Plenum press, p.67-102 (1967).

[16] Donald Ross, Mechanics of underwater noise, Peninsula Publishing Los Altos, California, p.159 (1987).

[17] L. Cohen, Time-Frequency distributions, Prentice Hall PTR, Englewood Cliffs, New Jersey 07632 (1995).

[18] F. Hlawatsch, Time-frequency analysis and synthesis of linear signal spaces, Kluwer academic publishers (1995).

[19] Leon Cohen, "Time-Frequency distributions- A review", *Proceedings of the IEEE*, **77**, No.7, p.941-981, July (1989).

[20] Jin-Ho Park, Yang-Hann Kim, "An impact source localization on an elastic plate in a noisy environment", Measurement science and technology, Vol. 17, No. 10, pp.2757-2766, 2006

[21] Jin-Ho Park, Yang-Hann Kim, "An impact source localization on a spherical shell using smoothed Wigner-Ville distributions", Key Engineering Materials, Vol. 321-323, pp. 1274-1279, 2006

[22] S.M. Ziola and M.R. Gorman, "Source location in thin plates using cross-correlation", J. Acoust. Soc. Am. 90(5), pp.2551-2556, 1991.

[23] J. M. Combes, A. Grossman, and P. Tchamitchian, Eds. 1989, Wavelets, Time-Frequency methods, and phase space, Berlin: Springer (1989).

[24] T.-G. Jeong, "Study on the non-stationary behavior of slider air bearing using reassigned time-frequency analysis", *The Korean Society for Noise and Vibration Engineering*, **16**, No. 3, p.255-262 (2006).

[25] Y.-K. Park and Y.-H. Kim, "A method to reduce the cross-talk of Wigner-Ville distribution; Rotating window", *The Korean Society for Noise and Vibration Engineering*, **7**, No. 2, p.319-329 (1997).

[26] Y.-K. Park and Y.-H. Kim, "Wigner-Ville distribution applying the rotating window and its characteristics," *The Korean Society for Noise and Vibration Engineering*, **7**, No. 5, p.747-756 (1997).